Comparison of Whole Body Transmit Coil Configurations for RF Shimming at 3T

K. Nehrke[1], U. Katscher[1], P. Börnert[1], and I. Graesslin[1]
[1]Philips Research Europe, Hamburg, Germany

Introduction

Whole body MRI at 3T may be impeded by B_1 transmit field inhomogeneities caused by the dielectric shortening of the RF wavelength [1]. RF shimming techniques based on parallel transmission [2,3] can strongly improve the image quality in clinical whole body applications [4]. In this context, it is an important question, how the RF shimming performance depends on the chosen coil topology and, in particular, on the number of transmit channels. In the present work, an 8-channel transmit system is used for B_1 mapping and shimming, providing the flexibility of emulating different coil configurations and comparing their RF shimming performance.

Methods

In vivo experiments (eleven healthy volunteers, all male, age: 27-49, BMI: 18-28) were performed on a 3T MRI system (Philips Healthcare, Best, The Netherlands) equipped with eight transmit channels [5] and an 8-element TX/RX TEM body coil [6]. The AFI (Actual Flip Angle Imaging) technique [7] was used for abdominal B_1 mapping (450×270×75 mm³ FOV, 64×38×5 matrix, angle = 60°, TR_1 = 20 ms, TR_2 = 100 ms, TE = 2.3 ms, transverse orientation, improved spoiling scheme [8], all-but-one coil encoding [9], resulting in 18 seconds scan time per 3D B_1 map, cf. Fig.1). For RF shimming, magnitude least square fitting (Fig.2) of the multi-coil maps was performed using a dedicated Java implementation of the local variable exchange method [10]. Tikhonov regularization was used to restrict the optimization to a selected set of coil eigenmodes. To enable or disable a certain coil eigenmode *i*, the corresponding regularization parameter λ_i was set to 0 or ∞, respectively. Four different eigenmode sets were compared: a) quadrature coil (λ_1=0), b) 2-port birdcage (quad and anti-quad, λ_1=λ_7=0) [11]), c) 4-channel coil setup proposed in ref. [12] ($\lambda_{1..4}$=0) and d) full 8 channels ($\lambda_{1..8}$=0). The coefficient of variation c_v= RMSD(B_1)/ RMS(B_1) of the synthesized shimmed maps was taken as homogeneity measure and compared to the quadrature case, which was chosen as a reference. In addition, the required total power ($\|\mathbf{b}\|^2$) and the maximum power per coil element ($\max\{b_i^2\}$) were determined from the fitted drive scales and normalized to the RMS(B_1) for the considered coil configurations.

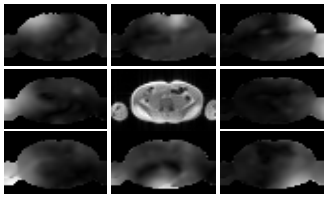

FIG.1. B_1 maps from the eight transmit channels are shown. The chosen target anatomy is shown in the centre. For clarity, the measured all-but-one maps were transformed to single-coil maps.

$$b = \arg_{b,z}\min\left\{\sum_{i\in w}\left|A_i b - m_i z_i\right|^2 + \left\|F\Lambda F^{-1} b\right\|_2^2\right\}\ ,\ \text{s.t.}\ |z_i| = 1$$

$$F_{k,l} = \exp\left(i2\pi(k-1)(l-1)/N\right)\ ,\ \Lambda = \begin{pmatrix}\lambda_1 & 0 & 0\\ 0 & \ddots & 0\\ 0 & 0 & \lambda_N\end{pmatrix}$$

FIG.2. **RF Shimming algorithm:** Mode-Selective magnitude Least-Squares fitting has been performed (*b*: drive scales, *A*: B_1 maps, *m*: target magnetization, Λ: regularization matrix for coil eigenmodes). The Fourier matrix *F* accounts for the fact that the employed transmit coil array is driven directly in "loop mode" (in contrast to the Butler matrix approach).

Results

RF shimming took about one second for each set of B_1 maps on a conventional PC. For the quadrature mode, significant shading artefacts became apparent in the shimmed B_1 maps (Fig.3). For the 2-channel configuration, the inhomogeneity was reduced by 27% on average. For the considered 4-channel configuration, the relative improvement was slightly worse (26%). Finally, the 8-channel configuration yielded 49% reduction of B_1 homogeneity. The total RF power decreased slightly for the 2-channel configuration (-9%) and increased slightly for the 4- and 8-channel configurations (+5% and +6%, respectively). The maximum power per coil element increased by 33%, 50% and 108% for the 2-, 4-, and 8-channel configurations, respectively. The results show a relatively large scattering, which was attributed to the variability of the volunteer cohort with respect to the body shape [11].

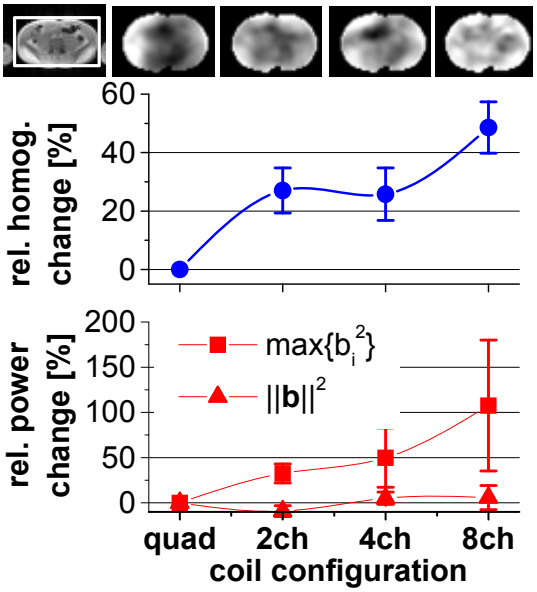

FIG.3. Shimmed B_1-maps of abdomen (top row) are shown for different transmit coil configurations (from left to right: quadrature, 2-channel, 4-channel and 8-channel). The white frame in the anatomical image shown at leftmost, indicates the target area used for shimming. The plots show the relative changes of B_1 homogeneitiy 1-$c_v/c_{v,quad}$ (●), maximum RF power per coil element (■) and total RF power (▲) for the different coil configurations normalized to the quadrature case and RMS(B_1).

Discussion

The results indicate that the RF shimming performance of the 2-port birdcage coil at 3T is slightly superior to the 4-channel configuration. Moreover, the 2-port birdcage coil achieves approx. 60% of the maximum uniformity improvement yielded by the 8-channel configuration. In practice, the improved shimming performance of the 8-channel configuration will not always be fully achievable, as a result of the significant power penalty, requiring some kind of additional regularization to stay within technically feasible power limits. Moreover, the additional degrees of freedom increase the complexity of the system, potentially making the scanner more expensive and less robust with respect to e.g. B_1 mapping, RF shimming, and hence, SAR control. Therefore, more in vivo evaluation based on different application scenarios is required to define more precise constraints and requirements. This should also include a systematic investigation of the impact of the body shape (e.g. body aspect ratio [11]) on the RF shimming performance.

References

[1] Kuhl CK. Radiology. 2007;244:929-30. **[2]** Katscher U et al. MRM 2003;49:144-50. **[3]** Zhu Y. MRM 2004;51:775-84. **[4]** Willinek WA et al. ISMRM 2009; p.4006. **[5]** Grässlin I et al., ISMRM 2006, p.129. **[6]** Vernickel P et al. MRM 2007;58:381-9. **[7]** Yarnykh VL. MRM 2007;57:192-200. **[8]** Nehrke K. MRM 2009;61:84-92. **[9]** Nehrke K et al. ISMRM 2008. P.353. **[10]** Setsompop K et al. MRM 2008;59:908-15. **[11]** Zhai Z et al. ISMRM 2009. p.3045. **[12]** Nistler J et al. ISMTM 2006. P.2471.